

The redshift-space power spectrum in the halo model

Martin White[★]

Harvard-Smithsonian Center for Astrophysics, 60 Garden Street, Cambridge, MA 02138, USA

Accepted 2000 August 9. Received 2000 July 21; in original form 2000 May 10

ABSTRACT

Recently there has been a lot of attention focused on a virialized halo-based approach to understanding the properties of the matter and galaxy power spectrum. We show that this model allows a natural treatment of the large- and small-scale redshift-space distortions, which we develop here, which extends the pedagogical value of the approach.

Key words: cosmology: theory – large-scale structure of Universe.

1 INTRODUCTION

The power spectrum of the mass fluctuations in the Universe is one of the most fundamental quantities in large-scale structure. It is robust, but sensitive to several cosmological parameters such as the Hubble constant, the matter density and of course the primordial power spectrum (usually parametrized by an amplitude and a slope). While the theory behind the power spectrum in the linear regime is quite straightforward, analytically handling clustering in the non-linear regime has proven quite difficult. Recently several authors (Ma & Fry 2000; Seljak 2001; Peacock 2000; Peacock & Smith 2000) have developed a new way of looking at the non-linear power spectrum which imagines all the mass in the Universe lies in a halo of some mass (Press & Schechter 1974). They postulate that on large scales the haloes cluster according to linear theory while on small scales the power is dominated by the halo profiles (Neyman, Scott & Shane 1953; Peebles 1974). Specifically most pairs of dark matter particles with small inter-particle separations lie within the same halo, and thus their correlations can be predicted by the halo profile. While this model requires many ingredients to be fixed by numerical experiments (typically N -body simulations) it provides a useful structure for thinking about gravitational clustering which gives insights into several outstanding problems (Seljak 2000; Peacock & Smith 2000; Seljak, Burwell & Pen 2001; Atrio-Barandela & Muckel 1999; Cooray, Hu & Miralda-Escude 2000).

The work to date has all focused on the clustering of the matter or galaxies in ‘real space’, whereas many if not most observations of clustering take place in ‘redshift space’. It is the purpose of this work to show that redshift-space distortions can be handled naturally in the halo picture and that doing so provides insight into some well-studied phenomena.

2 THE HALO MODEL

The model for non-linear clustering is based on the Press–Schechter (1974) theory, in which all of the mass in the Universe

resides in a virialized halo of a certain mass. The extensions to this theory introduced recently allow one to calculate the power spectra and cross-correlations between both the mass and the galaxies, given a suitable prescription for how galaxies populate dark matter haloes. Since at present such prescriptions are somewhat ad hoc we shall concentrate here on the mass power spectrum, though there is no obstacle in principle to extending the method to galaxies.

In this model the power spectrum, $P(k)$, is the sum of two pieces. The first is that owing to a system of (smooth) haloes of profile $y(k)$ laid down with inter-halo correlations assumed to be a biased sampling of $P_{\text{lin}}(k)$. Since the real-space convolution is simply a Fourier-space multiplication this contribution is

$$P^{2\text{-halo}}(k) = P_{\text{lin}}(k) \left[\int f(\nu) d\nu b(\nu) y(k; M) \right]^2, \quad (1)$$

where $b(\nu)$ is the (linear) bias of a halo of mass $M(\nu)$ and $f(\nu)$ is the multiplicity function. The peak height ν is related to the mass of the halo through

$$\nu \equiv \left[\frac{\delta_c}{\sigma(M)} \right]^2, \quad (2)$$

where $\delta_c = 1.69$ and $\sigma(M)$ is the rms fluctuation in the matter density smoothed with a top-hat filter on a scale $R^3 = 3M/4\pi\bar{\rho}$. Both b and f come from fits to N -body simulations. We use (Sheth & Tormen 1999)

$$b(\nu) = 1 + \frac{\nu - 1}{\delta_c} + \frac{2p}{\delta_c(1 + \nu^p)} \quad (3)$$

and

$$\nu f(\nu) = A(1 + \nu'^{-p})\nu^{1/2} e^{-\nu'^2/2}, \quad (4)$$

where $p = 0.3$ and $\nu' = 0.707\nu$. The normalization constant A is fixed by the requirement that all of the mass lie in a given halo

$$\int f(\nu) d\nu = 1. \quad (5)$$

We assume that the haloes all have spherical profiles depending

[★] E-mail: mwhite@cfa.harvard.edu

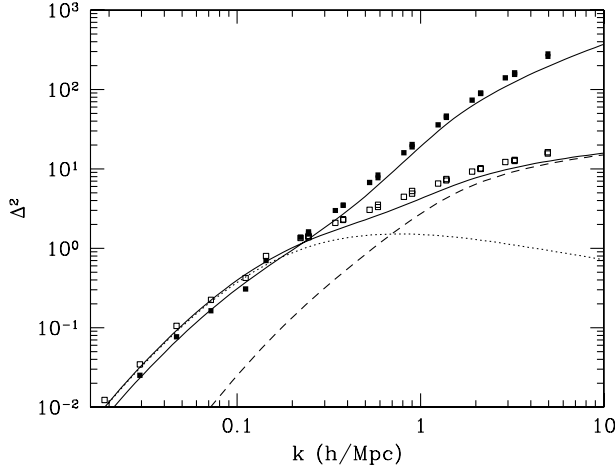


Figure 1. The predictions of the halo model for real- and redshift-space clustering, compared to a sequence of N -body simulations. The upper solid line is the sum of equations (1) and (10). The solid squares show the results of N -body simulations. The lower solid line is the prediction for the redshift-space power spectrum (equation 16) and the open squares the N -body results. The contribution of the 2-halo (dotted) and 1-halo (dashed) terms to the total is also shown.

only on the mass. We neglect any substructure or haloes-within-haloes as this seems to be unimportant for the power spectrum. We take the ‘NFW’ form (Navarro, Frenk & White 1996)

$$\rho(r) = \frac{\rho_0}{x(1+x)^2}, \quad (6)$$

where $x = r/r_s$ is a scaled radius, although our results are not particularly sensitive to this choice (Seljak 2000). The mass of this halo is defined to be the virial mass $M = (4\pi/3)\delta_{\text{vir}}\bar{\rho}r_{\text{vir}}^3$ where we take $\delta_{\text{vir}} = 200$ and define the virial radius, r_{vir} , as the radius within which the mean density enclosed is δ_{vir} times the background density.¹ The concentration parameter $c = r_{\text{vir}}/r_s$. The profile can then be described by its virial mass and concentration. N -body simulations suggest the two are related and we follow (Seljak 2000) in using

$$c(M) = 10 \left(\frac{M}{M_*} \right)^{-0.2}, \quad (7)$$

where $\sigma(M_*) = 1$.

Finally then we need $y(k)$ which is the Fourier transform of equation (6) normalized to unit mass. The Fourier transform can be done analytically

$$\bar{\rho}(k) = 4\pi\rho_0 r_s^3 \left[\cos z \{ \text{Ci}[(1+c)z] - \text{Ci}(z) \} + \sin z \{ \text{Si}[(1+c)z] - \text{Si}(z) \} - \frac{\sin cz}{(1+c)z} \right], \quad (8)$$

where $z \equiv kr_s$ and the total mass is

$$M = 4\pi\rho_0 r_s^3 \left[\log(1+c) - \frac{c}{1+c} \right]. \quad (9)$$

¹ In principle this is cosmology dependent, and for $\Omega_{\text{mat}} = 0.3$ should be closer to 300, but we follow (Seljak 2000) in holding δ_{vir} fixed and refer the reader to the discussion in that paper.

Equation (1) is the dominant contribution to the power spectrum on large scales. On small scales we are dominated by pairs lying within a single halo

$$P^{1\text{-halo}}(k) = \frac{1}{(2\pi)^3} \int f(\nu) d\nu \frac{M(\nu)}{\bar{\rho}} |y(k)|^2. \quad (10)$$

We show an example of how well this formalism predicts the matter power spectrum at $z=0$ in Fig. 1. We have chosen a particular Λ CDM model with $\Omega_m = 0.3$, $\Omega_\Lambda = 0.7$, $h = 0.7$, $\Omega_B h^2 = 0.02$ and $n = 1$. The model has been normalized to the *COBE* four-year data using the method of Bunn & White (1997). The agreement in the linear regime is good, as is to be expected. On smaller scales the model is a surprisingly good fit to the N -body data given the simplicity of the assumptions. The slight shortfall in power at higher k can be remedied by modifying the prescription somewhat, but we will here stick to the parameters outlined in (Seljak 2001) – this model is valuable more for its pedagogical value than as a substitute for direct calculations.

3 REDSHIFT-SPACE DISTORTIONS

The model described above naturally lends itself to a treatment of redshift-space distortions. There are two effects that come in when moving to redshift space. The first is a boost of power on large scales owing to streaming of matter into overdense regions. The second is a reduction of power on small scales owing to virial motions within an object. In the halo model the large-scale and small-scale effects can be separated out in a simple fashion.

Kaiser (1987) first showed that on large scales one expects an enhancement of the power spectrum in redshift space. In linear theory a density perturbation δ_k generates a velocity perturbation $\delta = -ikv$ with v parallel to k . Using density conservation to linear order and making the distant observer approximation [$kr \gg 1$, we shall work throughout in the plane-parallel limit, see (Heavens & Taylor 1995; Szalay, Matsubara & Landy 1998) for a large-angle formalism] the redshift-space density contrast can be written as

$$\delta_{\text{redshift}} = \delta_{\text{real}}(1 + f\mu^2), \quad (11)$$

where $f(\Omega) \equiv d \log \delta / d \log a \approx \Omega^{0.6}$, a is the scale-factor and $\mu = \hat{r} \cdot \hat{k}$. Thus on large-scales the power spectrum is increased by

$$\frac{1}{2} \int_{-1}^{+1} d\mu (1 + f\mu^2)^2 = 1 + \frac{2}{3}f + \frac{1}{5}f^2, \quad (12)$$

which is approximately 1.37 in our model.

On small scales virial motions within collapsed objects reduce power in redshift space. If we assume that our haloes are isotropic, virialized and isothermal with 1D velocity dispersion σ then the peculiar motions *within* the halo add a Gaussian noise to the redshift-space radial coordinate. Once again the real-space convolution becomes a Fourier-space multiplication and the inferred density contrast is

$$\delta_{\text{redshift}} = \delta_{\text{real}} e^{-(k\sigma\mu)^2/2}. \quad (13)$$

Integrating this over μ gives a suppression

$$\mathcal{R}_1(y = k\sigma) = \sqrt{\frac{\pi}{2}} \frac{\text{erf}(y/\sqrt{2})}{y}. \quad (14)$$

As pointed out by Peacock & Dodds (1994) however, the ‘full’ effect of redshift-space distortions includes both the enhancement and the suppression of power, and one must include the μ dependence of both factors before performing the integral.

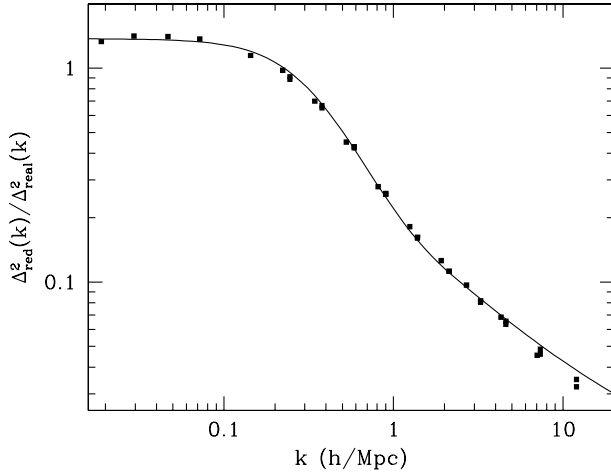


Figure 2. The ratio of power in redshift space, compared to real space, from the halo model (solid line) and from N -body simulations (points).

Including both terms the redshift-space distortion becomes, upon integrating over μ ,

$$\mathcal{R}_2(y = k\sigma) = \frac{\sqrt{\pi} \operatorname{erf}(y)}{8 y^5} [3f^2 + 4fy^2 + 4y^4] - \frac{e^{-y^2}}{4y^4} [f^2(3 + 2y^2) + 4fy^2] \quad (15)$$

Thus to predict the redshift space power spectrum in the halo model we modify equations (1) and (10) to

$$P(k) = \left(1 + \frac{2}{3}f + \frac{1}{5}f^2\right) P_{\text{lin}}(k) \times \left[\int f(\nu) d\nu b(\nu) \mathcal{R}_1(k\sigma) y(k; M) \right]^2 + \frac{1}{(2\pi)^3} \int f(\nu) d\nu \frac{M(\nu)}{\bar{\rho}} \mathcal{R}_2(k\sigma) |y(k)|^2. \quad (16)$$

In the first term we have broken out the enhancement owing to halo motions, treated in linear theory, and the \mathcal{R}_1 term from the virial motion. Technically we should perform the integral over ν including the Gaussian from equation (13) first and then integrate over μ (or keep the μ dependence explicit here and replace the prefactor with equation (11) if fitting the angular dependence). We can see in Fig. 2, however, that this numerically simpler approximation works quite well. Note that in contrast to the real-space power spectrum the clustering term remains significant to larger k .

We assume that the haloes are isothermal. From the mass within the virial radius the 1D velocity dispersion of a halo of mass M is

$$\sigma^2 = GM/2r_{\text{vir}} \quad (17)$$

$$= G \left(\frac{\pi}{6} M^2 \bar{\rho} \delta_{\text{vir}} \right)^{1/3}. \quad (18)$$

We find that our results are almost entirely unchanged if we estimate σ from the circular velocity interior to r_s instead of r_{vir} .

Putting the pieces together gives the lower solid line in Fig. 1. Notice that the model provides an adequate description of the redshift-space power spectrum. The clustering term remains significant to smaller scales, which may explain why perturbation theory results seem to work better in redshift space than in real space and why the redshift-space power spectrum approximates

the linear theory prediction over such a wide range of scales. At small- k this model makes the same predictions as linear theory with a constant ‘effective’ bias

$$\langle b \rangle \equiv \int f(\nu) d\nu b(\nu). \quad (19)$$

The high- k behaviour of the model qualitatively reproduces the suppression seen in the N -body simulations. This is not surprising since Sheth (1996) and Diaferio & Geller (1996) have shown that a sum of Gaussian random velocities weighted by the Press–Schechter (1974) mass function provides a good description of the exponential distribution of velocities seen in N -body simulations.

The model underestimates the N -body results in Fig. 1 in both real and redshift space. We show the prediction for the ratio of redshift-space to real-space power in Fig. 2 compared to the same ratio from the N -body simulations. Here we see that the agreement is very good over more than two decades in length-scale.

4 CONCLUSIONS

Many of the features of the power spectrum of density fluctuations in the Universe can be simply understood in a model based on virialized haloes. Important ingredients in the model are that the haloes be biased tracers of the linear power spectrum and have a uniform profile with a correlation between the internal structure and the mass which should span a wide range sampling a Press–Schechter (1974) like mass function. Within this model it is easy to account accurately for redshift-space distortions which alter the power on large and small scales. The effects of virialized motions within haloes suppress the ‘Poisson’ or 1-halo term, so the redshift-space power spectrum traces the linear theory result to smaller physical scales. This effect could be responsible for the fact that perturbation theory is known to work better in redshift space than real space when compared with numerical simulations.

ACKNOWLEDGMENTS

I thank U. Seljak and R. Sheth for useful comments on the manuscript. This work was supported by a grant from the US National Science Foundation.

REFERENCES

- Atrio-Barandela F., Muckel J. P., 1999, *ApJ*, 515, 465
- Bunn E., White M., 1997, *ApJ*, 480, 6
- Cooray A. R., Hu W., Miralda-Escude J., 2000, *ApJ*, 535, L9
- Diaferio A., Geller M. J., 1996, *ApJ*, 467, 19
- Heavens A. F., Taylor A. N., 1995, *MNRAS*, 275, 483
- Kaiser N., 1987, *MNRAS*, 227, 1
- Ma C.-P., Fry J. N., 2000, *ApJ*, 531, 87
- Navarro J., Frenk C. S., White S. D. M., 1996, *ApJ*, 462, 563
- Neyman J., Scott E. L., Shane C. D., 1953, *ApJ*, 117, 92
- Peacock J. A., 2000, Lectures at the NATO ASI, Structure Formation in the Universe. Cambridge, August 1999 (astro-ph/0002013)
- Peacock J. A., Dodds S. J., 1994, *MNRAS*, 267, 1020
- Peacock J. A., Smith R. E., 2000, *MNRAS*, in press [astro-ph/0005010]
- Peebles P. J. E., 1974, *A&A*, 32, 197
- Press W., Schechter P., 1974, *ApJ*, 187, 425
- Seljak U., 2001, preprint [astro-ph/0001493]
- Seljak U., Burwell J., Pen U.-L., 2001, preprint [astro-ph/0001120]
- Sheth R., 1996, *MNRAS*, 279, 1310
- Sheth R., Tormen G., 1999, *MNRAS*, 308, 119
- Szalay A., Matsubara T., Landy S. D., 1998, *ApJ*, 498, L1

This paper has been typeset from a \LaTeX file prepared by the author.